Experimental Observations of Breathing Dissipative Soliton Explosions

Junsong Peng and Heping Zeng*

State Key Laboratory of Precision Spectroscopy, East China Normal University, Shanghai 200062, China

(Received 18 December 2018; revised manuscript received 18 June 2019; published 26 September 2019)

Solitons are revealed to undergo sudden structural collapse upon nonlinear propagation and robust recurrence to the original state afterwards. Such fascinating dynamics, termed soliton explosions, are ubiquitous in dissipative systems, but, surprisingly, are, so far, found exclusively in parameter-invariant stationary solitons. Many nonlinear systems support dynamic solutions, such as breathing dissipative solitons (DSs), the energy and duration of which experience periodic evolutions. It is of fundamental importance to unveil whether breathing DSs also exhibit explosive dynamics. Here, we report on experimental observation of breathing DS explosions in mode-locked fiber lasers. A bifurcation diagram clearly shows how different laser regimes, including breathing DS explosions, breathing DSs, and continuous-wave mode locking, are switched by varying the pump power. While soliton explosions are found above the pump power for generating stable solitons, breathing DS explosions occur under the pump power to support stable breathing DSs. Nonlinearity-mediated giant Q-switching is critical to stimulate breathing DS explosions. Moreover, rogue waves are observed during breathing DS explosions. A correlation analysis shows that the spectral correlation evolves during breathing DS explosions from a low value at the explosion phase to a high one at the revival phase. Our results can contribute to the design of ultrafast lasers and are conducive to understanding the complex dynamics of nonlinear systems.

DOI: 10.1103/PhysRevApplied.12.034052

I. INTRODUCTION

The investigation of wave instabilities in mode-locked lasers is a fast-growing field, which can advance our general understanding of complex nonlinear systems [1–6]. Although a dissipative soliton (DS) can propagate without changes in dispersion and diffraction media, under certain conditions, it can explode into pieces, but recover to its original state later. This striking phenomenon is dubbed a soliton explosion, which was first predicted in 2000 [7]. Cundiff *et al.* first experimentally observed soliton explosions in a mode-locked Ti:sapphire laser [8].

In contrast to parameter-invariant stationary solitons, the energy and duration of breathers experience periodic evolutions. In the case of dissipative systems, the term breathing dissipative soliton is introduced [9]. In fact, real-world physical systems are generally dissipative. Breathing DSs have been investigated in various physical systems, such as optics [2,9–14], water waves [15–17], acoustics [18], and plasmas [19]. Breathing DSs constitute an important context of nonlinear science. They are strongly linked with the Fermi-Pasta-Ulam recurrence [11,20] and rogue waves [2]. Akin to solitons, multiple breathing DSs can also form molecules (breather wave molecules) [21]. Breathing DSs such as Peregrine solitons [22] are regarded as prototypes of rogue waves. Rogue waves with even larger amplitudes can be generated via breathing DS collisions [23–25]. From points of view in fundamental physics, breathing DSs link two distinguished regimes of nonlinear propagation: plane-wave modulation instability and high-power pulse propagation [13,26]. Continuous interest in breathing DSs is also stimulated by their practical applications. For instance, breathing DSs can increase the resolution of a dual-comb source [27].

It is of fundamental significance to know whether breathing DSs exhibit explosive dynamics akin to solitons. So far, only solitons are found to exhibit explosive dynamics. The lack of observation of explosions of any other nonlinear waves raises the significant question of whether explosion is a unique characteristic of solitons. Breathing DSs provide an opportunity to address this question. The lack of observations of breathing DS explosions is because of two reasons. First, studies on soliton explosions imply that dissipation plays an important role. Previous investigations on breathing DSs were generally conducted in conservative systems where dissipation was negligible. Second, explosions are nonrepetitive fast events, while standard measurement tools are too slow to record such fast dynamics.

Here, we report on the first observation of breathing DS explosions in a dissipative system: a mode-locked fiber laser. Breathing DSs periodically change their spectra over consecutive roundtrips (RTs) of the laser. However, they suddenly collapse, but revive after certain RTs.

*hpzeng@phy.ecnu.edu.cn

In contrast to soliton explosions, which emerge when the pump level of a laser is higher than that for stable solitons, breathing DS explosions occur when the pump level is lower than that for breathing DSs. Nonlinearity-mediated giant Q-switching is the mechanism that triggers breathing DS explosions. Furthermore, breathing DS explosions can generate rogue waves. A spectral correlation analysis method previously developed for random lasing [28] is used here to characterize the evolution of spectral correlation during breathing DS explosions. These transient dynamics are observed by virtue of real-time spectral measurements, dispersive Fourier transformation (DFT) [29].

II. RESULTS

A. Experimental setups

Figure 1 shows the configuration of the laser. The laser has a length of 10.5 m. It consists of three types of fibers: a single-mode fiber, a DCF, and an EDF. The laser has a net normal dispersion. The laser output is divided into two ports via an optical coupler. One port (without stretching) is to record the evolution of the instantaneous intensity, $I(t)$, realizing spatiotemporal intensity measurements [30,31]. The other port contains a long dispersive fiber (approximately 11 km in our experiments) to implement DFT measurements [29,32]. DFT utilizes dispersion to map the spectrum of a pulse to a temporal waveform, which imitates the pulse spectrum. Therefore, DFT can record the spectrum in real time. DFT has a wide range of applications in diverse fields [33]. For example, DFT helps to reveal the build-up of mode locking [5,6,34] and soliton molecules [35,36], internal motion of soliton molecules [3,4], triple-state dissipative soliton switching [37], and soliton explosions [38–41]. Two identical photodetectors with a bandwidth of 50 GHz (PD1, PD2) are employed and the signals are measured by a real-time oscilloscope with a sampling rate of 80 GSa/s and 33 GHz bandwidth. Synchronous measurements of the spectral and temporal intensities of the output pulses are realized by measuring the delay between the two photodetectors.

B. Experimental observation of breathing DS explosions

The fiber laser is mode-locked through the standard mechanism of nonlinear polarization rotation. After initiating mode locking by rotating the polarization controllers under an appropriate pump level, we reveal the mode-locking dynamics by varying the pump levels. The laser can work on three typical mode-locking regimes: stable mode locking, breathing DS mode locking, and breathing DS explosions. Starting from the stable mode-locking regime, decreasing the pump power can make the laser switch to the breathing DS mode-locking regime. An optical spectrum analyzer (OSA) is not able to resolve the fast dynamics of breathing DSs. DFT can measure optical spectra in real time. Figure 1(b) shows the roundtrip-resolved spectra of the breathing DSs measured by DFT, which evolve periodically. The accuracy of DFT is confirmed by comparing the averaged DFT spectra (black) with the one measured by OSA (red), as shown in Appendix A. The related pulse energy also exhibits periodic evolution, as shown in Fig. 1(b) (white line). Figure 1(c) is a magnified version of Fig. 1(b), which is discussed in Sec. II C.

Remarkably, by decreasing the pump power from the breathing DS mode-locking regime, breathing DS explosions emerge. It is beyond the resolution of the

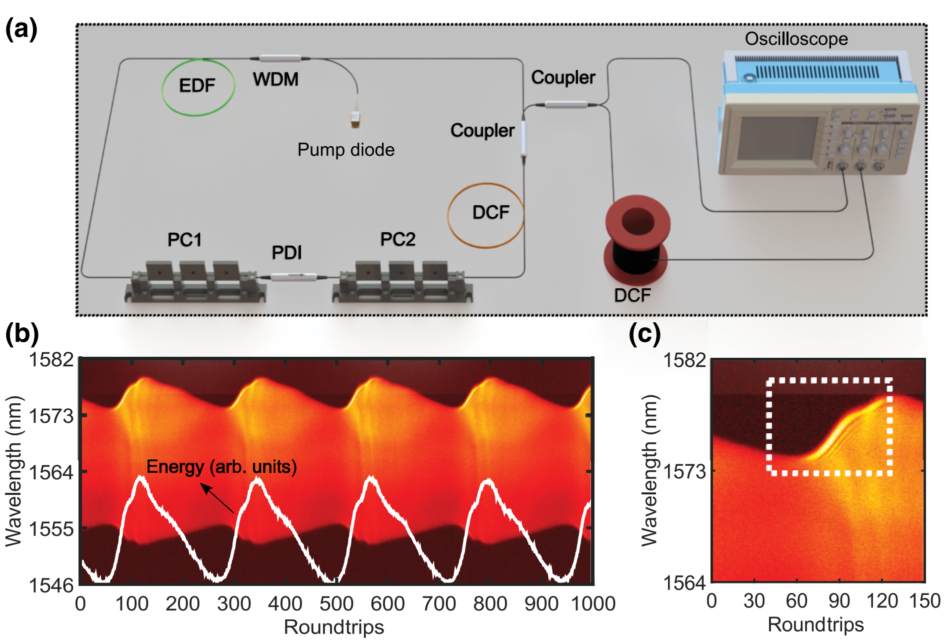

FIG. 1. (a) Setup of the laser and detection system. WDM: wavelength-division multiplexer; EDF: erbium-doped fiber; PC: polarization controller; PDI: polarization-dependent isolator; DCF: dispersion-compensating fiber; PD: photodetector. (b) Periodic spectral evolution of breathing dissipative solitons measured by DFT; the white line depicts the energy evolution. (c) A magnified region where fringes appear in (b).

photodetector to resolve the fine structures of the exploded breathing DS in the temporal domain. Alternatively, such events can be identified in the spectral domain by virtue of DFT, as widely used in unveiling the dynamics of soliton explosions [38–41]. The spectral evolution of the breathing DS explosion regime measured by DFT is depicted in Fig. 2(a). In contrast to stable breathing DSs [Fig. 1(b)], Fig. 2(a) shows vastly different dynamics. In this case, the instabilities of breathing DSs can be clearly observed. Periodic spectral evolution of breathing DSs are disrupted by wide and chaotic spectra, which evidence explosions of breathing DSs. Weak and narrow spectra lie between them.

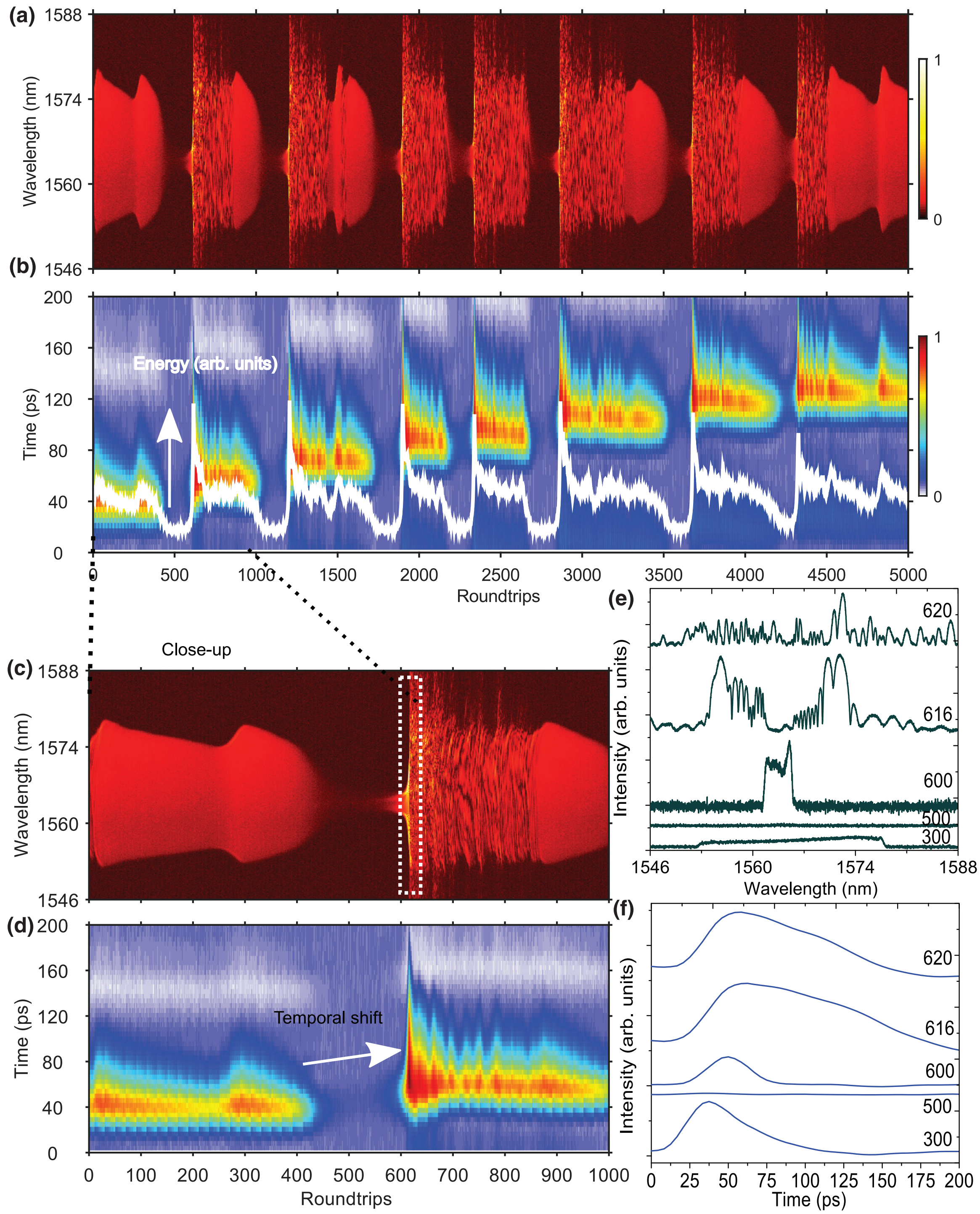

FIG. 2. Breathing DS explosions. (a) Spectral evolution over consecutive roundtrips. (b) Synchronous temporal intensity evolution; the white line shows the energy evolution. (c) A close-up of (a). (d) A close-up of (b). (e) Five representative cross sections in (c), at roundtrip numbers of 300, 500, 600, 616, and 620. (f) Five representative cross sections in (d).

The synchronous temporal intensity evolutions are shown in Fig. 2(b).

To investigate breathing DS explosions in detail, Figs. 2(a) and 2(b) are magnified from RT numbers of 0 to 1000, as shown in Figs. 2(c) and 2(d). The spectral and temporal intensities change significantly, as illustrated in Figs. 2(c) and 2(d). Five typical spectral and temporal profiles are shown in Figs. 2(e) and 2(f), which are the cross sections of Figs. 2(c) and 2(d) at RT numbers of 300, 500, 600, 616, and 620. The spectrum is quite broad at a RT number of 300. There are nearly no spectral components at a RT number of 500 [Fig. 2(e)], which is also confirmed by the corresponding nearly zero temporal intensity at that RT [Fig. 2(f)]. However, the weak pulse grows gradually thereafter, giving rise to a stronger pulse at a RT number of 600 [Figs. 2(e) and 2(f)]. This pulse is unstable and explosions start at around a RT number of 616. Two representative spectral profiles referring to explosions are shown at RT numbers of 616 and 620. The chaotic spectra then gradually narrow to coherent ones (RTs 600–900); this indicates the revival of breathing DSs.

Nonsymmetrical temporal intensity profiles are observed during breathing DS explosions. Two examples are shown in Fig. 2(f) at RT numbers of 616 and 620. The asymmetric temporal intensity profiles may be understood as follows. Since the pulse is positively chirped (a characteristic of mode-locked normal-dispersion fiber lasers), the pulse leading edge has a lower frequency component. These components travel faster than the higher frequency components because the net dispersion of the laser is normal, resulting in a long tail. Figure 2(b) shows that there are temporal shifts in breathing DS explosions. The breathing DS shifts by 80 ps over 5000 RTs. The temporal shift arises from the weak pulse, which can be observed from RT numbers of 400 to 600 [Fig. 2(d)], as denoted by the white arrow. Temporal shifts are also observed in soliton explosions [38,39].

Energy evolutions give further insights, as shown in Fig. 2(b) (white line). The energy decreases to a stationary value for weak pulses [RTs 400–600, Fig. 2(c)]; however, it suddenly increases to a maximum value once breathing DS explosion takes place at around 600 RTs. The energy decreases in the late stage of breathing DS explosions (RTs 600–860). The energy decrease arises from two dissipative effects. First, the spectra of the exploded breathing DSs are quite broad in the beginning (42 nm, from 1544 to 1586 nm), as shown in Fig. 2(e) (RT 620); thus, the EDF with a narrow-gain bandwidth dissipates the pulse energy by filtering. This mechanism is supported by the fact that the spectral bandwidth of the pulse decreases gradually during breathing DS explosions [RTs 600–860, Fig. 2(c)]. Second, an explosion means a pulse explodes into many pieces temporally [7], although it is beyond the resolution of the detector to resolve these pieces over the time domain of our experiments. Therefore, these weak pieces experience loss from the saturable absorber, which has higher losses for weak pulses. A similar mechanism is observed in the build-up of mode locking in a fiber laser in which only the stronger pulse survives [6].

The detailed dynamics of each explosion event is similar in Figs. 2(a) and 2(b). The origins of breathing DS explosions are clear. Breathing DSs present periodic energy variations. In the phase of decreasing energy, the mode-locking mechanism imposes a large loss on the pulse, leading to a significant decrease in the pulse intensity in the cavity, as shown in Fig. 2(c) (RTs 400–600). Therefore, population inversion accumulates in the cavity, leading to a large *Q*-switching pulse in the laser [42]. The energy of the *Q*-switching pulse is so high that it results in broad chaotic spectra due to self-phase modulation (SPM). The development of SPM can be seen by magnifying the dashed box of Fig. 2(c), as shown in Fig. 3(a). Two cross sections are shown in Fig. 3(b) at RT numbers of 605 (black) and 615 (red). As the energy goes up, the spectrum becomes structured, as shown in the red curve [Fig. 3(b)]. Such structures are typical products of SPM [43,44]. The spectra collapse over the next RTs, meaning the occurring of breathing DS explosions. The *Q*-switching here is rather different from that of standard *Q*-switching because SPM is involved in the pulse dynamics. For standard *Q*-switched mode locking, nonlinear optical effects, such as SPM, are not involved in the laser dynamics [45].

A bifurcation diagram is conducive to identifying the transitions between different laser regimes. A well-known bifurcation in mode-locked lasers refers to the transition from *Q*-switching to continuous-wave (CW) mode locking, which is also confirmed by theoretical analysis [46]. Figure 4 is the bifurcation diagram showing the transitions between different regimes, including breathing DS explosions, stable breathing DS, and CW mode locking. The period of the breathing DS explosion regime refers to the period of explosion events. For CW mode locking, the period is zero. Real-time spectral evolutions of the pulses referring to the red points (*a*, *b*, *c*, and *d*) in Fig. 4 are shown in Appendix B. Real-time spectral evolutions of the pulses referring to the blue points in Fig. 4 are depicted in Figs. 1(b) and 2(a). The bifurcation diagram indicates how to enter different laser regimes by changing only the pump power.

C. Rogue waves in breathing DS explosions

Soliton explosions can induce rogue waves (RWs) [47]. It is of interest to know whether breathing DS explosions also relate to RWs. By virtue of DFT, RWs can be readily resolved in the spectral domain [48]. Recently, RWs detected in the spectral domain were termed spectral RWs [49]. Figure 5 shows the spectral intensity histograms of stable DSs, breathing DSs, and breathing DS explosions.

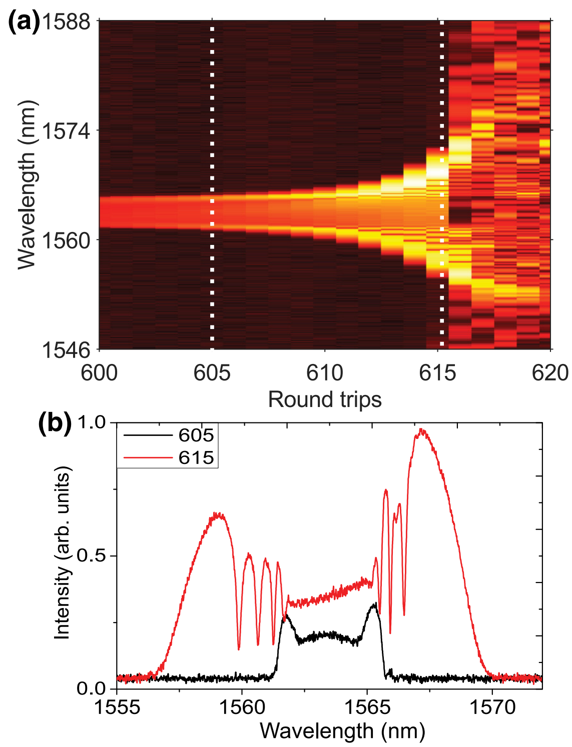

FIG. 3. (a) Magnified image of the dashed box in Fig. 2(c). (b) Two representative cross sections at roundtrip numbers of 605 (black) and 615 (red).

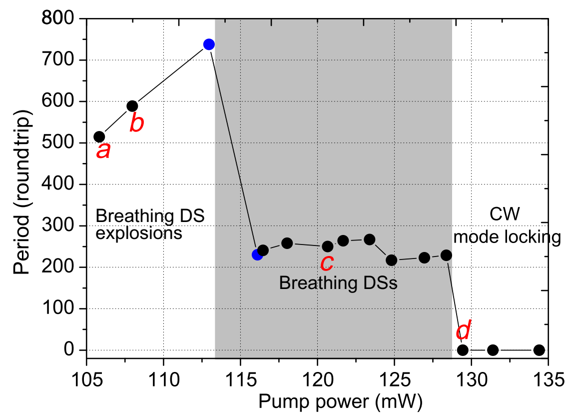

FIG. 4. A bifurcation diagram showing the transitions between breathing DS explosions, breathing DSs, and CW mode locking by varying only the pump power. Different regimes are distinguished by their periods.

The intensity (I) is normalized to the average intensity ($<I>$). The DFT data of 10 000 pulses are recorded in each regime and the maximum peak within each pulse is collected to compute the histogram, as shown in Fig. 5. For stable DSs, the intensity shows small fluctuations [Fig. 5(a)], in contrast to the other two [Figs. 5(b) and 5(c)]. The intensity distribution of the breathing DS regime [Fig. 5(b)] is similar to that of the breathing DS explosion regime [Fig. 5(c)]. The long tails (high intensities) in Fig. 5(b) refer to spectral peaks in Fig. 1(b) [a magnified version is shown in Fig. 1(c)]. One can see the development of fringes at the edges of the spectrum (around 1573 nm), which relate to shock-wave dynamics occurring in normal-dispersion mode-locked fiber lasers [50]. Significant wave height (I_{SWH}) is defined as the average amplitude of the highest third of the waves (denoted by the black lines in Fig. 5), and extreme events with amplitude of more than two times the I_{SWH} are RWs. The tails in Fig. 5(b) do not refer to RWs because they appear regularly, as seen in Fig. 1(b). In contrast, breathing DS explosions occur irregularly and the position of the maximum peak is random within a pulse. Therefore, RWs are only generated in the regime of breathing DS explosions and they arise mainly from SPM. The origins of RWs depend on the optical systems studied. While collisions of breathing DSs [23,25] and higher-order effects [48], such as third-order dispersion and stimulated Raman scattering, play important roles in RW formation in quasi-conservative systems, here our work shows that breathing DS explosions can generate RWs in a laser.

D. Correlations in breathing DS explosions

It seems that the spectra are rather noisy in the beginning of breathing DS explosions [600–700 RTs, Fig. 2(c)] and become less noisy in the late stage (700–900 RTs). Yet, there are no tools to quantify these spectral dynamics. We employ a correlation analysis method previously used to quantify spectral correlation statistics in random lasing [28], to characterize the spectral correlation dynamics here. The correlation may be calculated by the overlap of the spectral intensity [28], $I_n(\lambda)$ and $I_{n+1}(\lambda)$, which are measured at consecutive RTs, n and $n+1$, defined as $C_{n,n+1} = \int I_n(\lambda) I_{n+1}(\lambda) d\lambda$ (subject to a normalization condition $C_{n,n} = C_{n+1,n+1} = 1$). A value of C close to zero represents distinct spectra over two consecutive RTs, while values close to one are retrieved for nearly identical spectra. Figure 6 shows the evolution of $C_{n,n+1}$ over consecutive RTs [calculated from Fig. 2(c)]. Before breathing DS explosion, $C_{n,n+1}$ has a value close to one, which confirms strong correlations between the laser emissions. The correlation fluctuates in the phase of explosion. It reaches a value close to unity when the breathing DS is revived. The revival of the breathing DS can arise from mode locking, which can shape chaotic fields into coherent ones [5,6]. A magnified version of the correlation evolutions, together with the corresponding spectral evolutions, are shown in Fig. 7, where Figs. 7(a) and 7(b) show the correlation and spectral evolutions from RT numbers 600 to 900, respectively. The correlation suddenly drops to a minimum value of 0.62 [the first arrow in Fig. 7(a)], signaling the onset of breathing DS explosions. The sudden decrease in the correlation arises from significant spectral

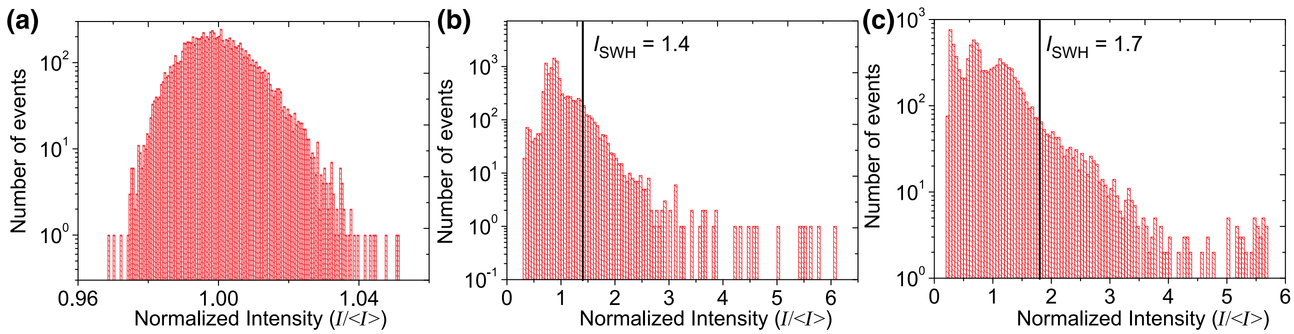

FIG. 5. Intensity histograms of the three mode-locking regimes. (a) Stable dissipative solitons. (b) Breathing dissipative solitons. (c) Breathing dissipative soliton explosions. The black line denotes the intensity of the significant wave height (I_{SWH}).

broadening (minimum spectral overlap) from RT numbers 615 to 616, as shown in Fig. 7(b) [see the magnified version in Fig. 3(a)]. Another two noticeable decreases in correlations around RT numbers of 660 and 780 are marked by two other black arrows in Fig. 7(a). The corresponding spectral evolutions reveal that they also mainly arise from abrupt spectral broadening [Fig. 7(b)]. The correlation has a high value at around a RT number of 720 [Fig. 7(a)], as the spectral lobes are broader and less noisy than those below 720 RTs [Fig. 7(b)]. The spectral analysis method can be extended to characterize correlations in soliton explosions and noiselike mode locking.

III. DISCUSSION

Our work can have both practical and fundamental applications. Although only stationary regimes of mode-locked fiber lasers are relevant for applications in many photonics systems, knowledge of nonstationary regimes are, nevertheless, also very important for practical applications. These instabilities are detrimental to applications. Knowing that they can happen and verifying the conditions for their occurrence are required before one can design systems or control laser parameters to avoid these instabilities. In this context, the first observations of breathing DS explosions and the bifurcation diagram, showing the transitions between breathing DS explosions, stable breathing DSs, and CW mode locking, are vital for active control of working regimes of mode-locked lasers. Our studies are conducted in mode-locked normal-dispersion fiber lasers. These lasers have excellent performances over those in the anomalous or zero dispersion regimes in pulse energies, quality, and durations [51]; they can greatly simplify chirped-pulse amplification systems when used as seed sources [52]. Our work finds that these widely used mode-locked normal-dispersion fiber lasers suffer from instabilities arising from breathing DS explosions. This finding will certainly contribute to improving the stability of these ultrafast lasers, by taking into account this previously overlooked instability in laser design.

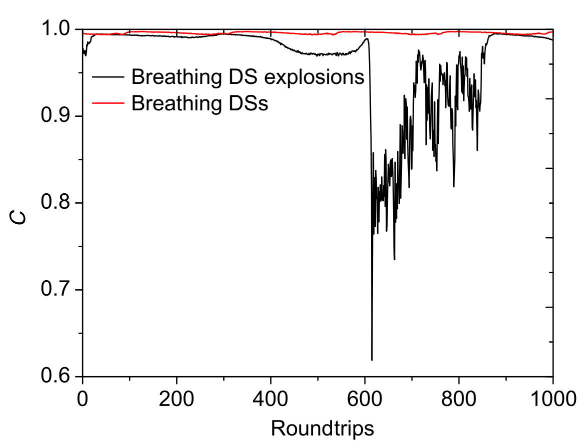

FIG. 6. The evolution of spectral correlations in the regimes of breathing DS explosions (black) and breathing DS (red), as calculated from data in Figs. 2(c) and 1(b), respectively.

Besides practical applications in laser optics, our results are also relevant for applications in fundamental science, such as extreme events. The generation mechanisms of RWs differ in distinct physical systems. Breathing DS collisions are responsible for rogue-wave generation in various systems [23–25]. Our work provides an alternative mechanism—breathing DS explosions—for understanding the origins of RWs. Our study contributes to this context by revealing that even a single breathing DS can generate RWs through breathing DS explosions. Such a mechanism could also prevail in water waves and passive fiber optics.

Soliton explosions have attracted considerable interest since the prediction of their existence [7]. The origins of soliton explosions are still under active investigation. Our work shows that nonlinearity-mediated Q-switching can trigger breathing DS explosions. Such a mechanism is also an alternative mechanism for the existence of soliton explosions. Our work, therefore, may be conducive to understanding soliton explosions as well.

Fiber lasers are well known for their versatile configurations, such as ring, linear, and theta cavities, as well as their compatibility with a rich variety of mode-locking mechanisms, including saturable absorbers based on various materials and multimode fibers. It is therefore of

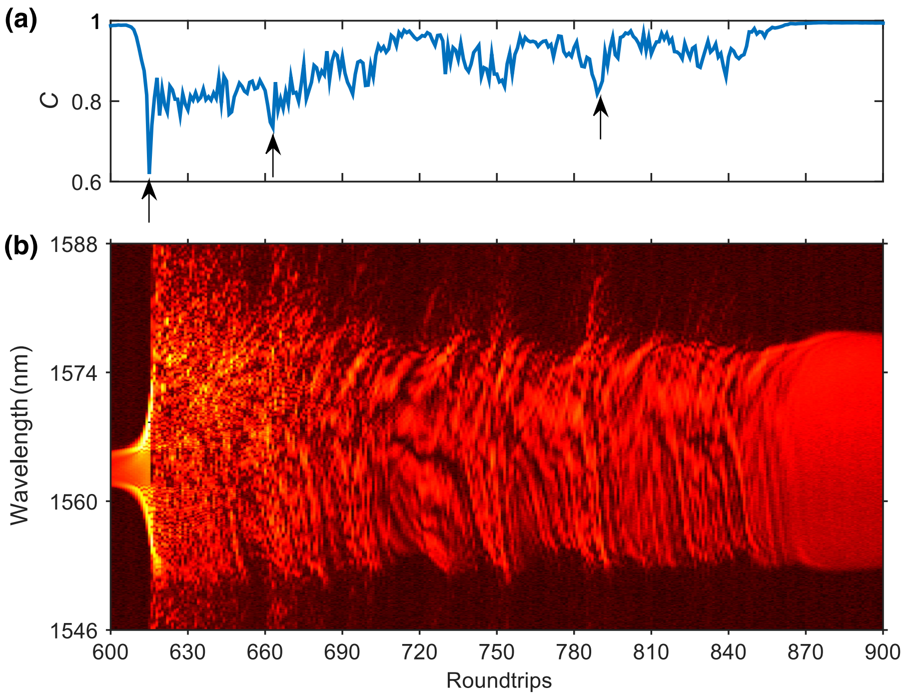

FIG. 7. (a) The evolution of spectral correlations from RT numbers 600 to 900 in Fig 2(c). (b) The corresponding spectral evolutions [a magnified version of Fig. 2(c)].

significant interest to explore breathing DS explosions in fiber laser cavities with different characteristics and operating conditions. Meanwhile, potentially, similar dynamics can also exist in ultrafast Ti:sapphire and semiconductor lasers. More generally, since breathing DSs are fundamental modes of many nonlinear dissipative systems, the dynamics we observe could open up the possibility of investigating breathing DS explosions in many physical systems.

IV. CONCLUSION

In conclusion, we find that, akin to solitons, breathing DSs can also exhibit explosions. This laser instability arises from nonlinearity-mediated giant *Q*-switching. Therefore, for practical applications where stable breathing DSs are preferred [27], the breathing DS explosion instability can be avoided by suppressing the *Q*-switching instability through feedback control [53,54]. This study will be our future work. There are many important nonlinear waves in optical systems, such as similaritons [55] and Nyquist pulses [56]. It is therefore of great interest to investigate whether these nontrivial pulses also show explosions. Moreover, we anticipate our work will also stimulate studies of breathing DS explosions in various other physical systems, especially in microresonators, where breathing DSs have been extensively investigated [9,11,12,57].

ACKNOWLEDGMENTS

This work is supported by the National Key Research and Development Program (Grant No. 2018YFB0407100), the National Natural Science Fund of China (Grants No. 11434005, No. 11727812, No. 11621404, No. 11561121003, No. 61775059, and No. 11704123), the Key Project of Shanghai Education Commission (Grant No. 2017-01-07-00-05-E00021), and the Science and Technology Innovation Program of Basic Science Foundation of Shanghai (Grant No. 18JC1412000).

APPENDIX A: ACCURACY OF DFT

The accuracy of DFT is confirmed by good agreement between the averaged spectra measured by DFT and the OSA, as shown in Fig. 8.

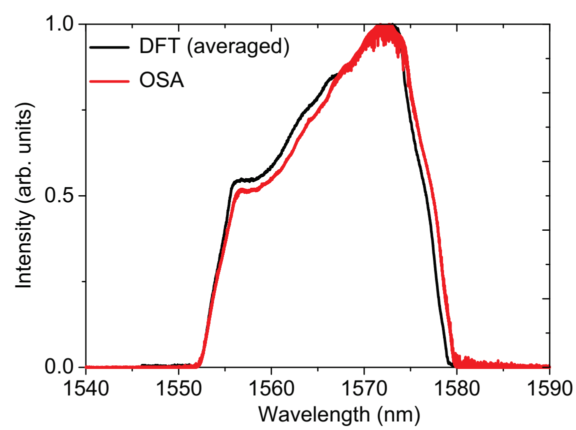

FIG. 8. Averaged spectra measured by DFT (black) and the OSA (red).

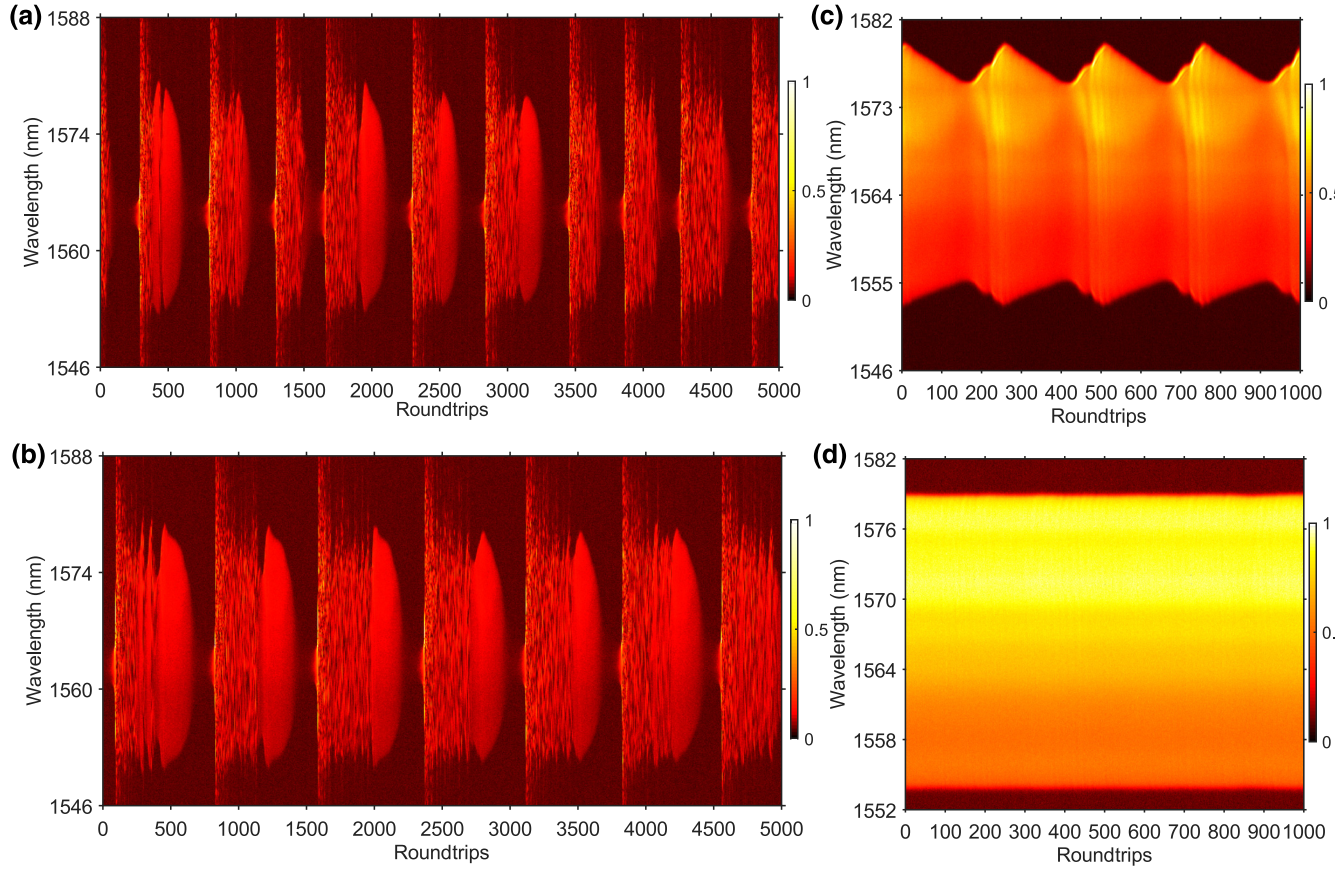

FIG. 9. Real-time spectral evolutions of pulses referring to points *a*, *b*, *c*, and *d* in Fig. 4.

APPENDIX B: SPECTRAL EVOLUTIONS OF THE DIFFERENT REGIMES IN THE BIFURCATION DIAGRAM

Here, more examples of real-time spectral evolutions of different laser regimes are depicted. Figure 9 shows the real-time spectral evolution of pulses referring to the red points (*a*, *b*, *c*, and *d*) in Fig. 4. The spectral evolution of the pulses referring to the blue points in Fig. 4 are shown in the main text [Figs. 1(b) and 2(a)].

[1] P. Grelu and N. Akhmediev, Dissipative solitons for mode-locked lasers, Nat. Photonics **6**, 84 (2012).

[2] J. M. Dudley, F. Dias, M. Erkintalo, and G. Genty, Instabilities, breathers and rogue waves in optics, Nat. Photonics **8**, 755 (2014).

[3] G. Herink, F. Kurtz, B. Jalali, D. R. Solli, and C. Ropers, Real-time spectral interferometry probes the internal dynamics of femtosecond soliton molecules, Science **356**, 50 (2017).

[4] K. Krupa, K. Nithyanandan, U. Andral, P. Tchofo-Dinda, and P. Grelu, Real-Time Observation of Internal Motion within Ultrafast Dissipative Optical Soliton Molecules, Phys. Rev. Lett. **118**, 243901 (2017).

[5] P. Ryczkowski, M. Närhi, C. Billet, J. M. Merolla, G. Genty, and J. M. Dudley, Real-time full-field characterization of transient dissipative soliton dynamics in a mode-locked laser, Nat. Photonics **12**, 221 (2018).

[6] J. Peng, M. Sorokina, S. Sugavanam, N. Tarasov, D. V. Churkin, S. K. Turitsyn, and H. Zeng, Real-time observation of dissipative soliton formation in nonlinear polarization rotation mode-locked fibre lasers, Commun. Phys. **1**, 20 (2018).

[7] J. M. Soto-Crespo, N. Akhmediev, and A. Ankiewicz, Pulsating, Creeping, and Erupting Solitons in Dissipative Systems, Phys. Rev. Lett. **85**, 2937 (2000).

[8] S. T. Cundiff, J. M. Soto-Crespo, and N. Akhmediev, Experimental Evidence for Soliton Explosions, Phys. Rev. Lett. **88**, 073903 (2002).

[9] E. Lucas, M. Karpov, H. Guo, M. L. Gorodetsky, and T. J. Kippenberg, Breathing dissipative solitons in optical microresonators, Nat. Commun. **8**, 736 (2017).

[10] B. Kibler, J. Fatome, C. Finot, G. Millot, F. Dias, G. Genty, N. Akhmediev, and J. M. Dudley, The Peregrine soliton in nonlinear fibre optics, Nat. Phys. **6**, 790 (2010).

[11] C. Bao, J. A. Jaramillo-Villegas, Y. Xuan, D. E. Leaird, M. Qi, and A. M. Weiner, Observation of Fermi-Pasta-Ulam Recurrence Induced by Breather Solitons in an Optical Microresonator, Phys. Rev. Lett. **117**, 163901 (2016).

[12] M. Yu, J. K. Jang, Y. Okawachi, A. G. Griffith, K. Luke, S. A. Miller, X. Ji, M. Lipson, and A. L. Gaeta, Breather

soliton dynamics in microresonators, Nat. Commun. **8**, 14569 (2017).

[13] A. Tikan, C. Billet, G. El, A. Tovbis, M. Bertola, T. Sylvestre, F. Gustave, S. Randoux, G. Genty, P. Suret, and J. M. Dudley, Universality of the Peregrine Soliton in the Focusing Dynamics of the Cubic Nonlinear Schrödinger Equation, Phys. Rev. Lett. **119**, 033901 (2017).

[14] S. Chen, Y. Ye, J. M. Soto-Crespo, P. Grelu, and F. Baronio, Peregrine Solitons Beyond the Threefold Limit and Their Two-Soliton Interactions, Phys. Rev. Lett. **121**, 10410 (2018).

[15] A. Chabchoub, Tracking Breather Dynamics in Irregular Sea State Conditions, Phys. Rev. Lett. **117**, 144103 (2016).

[16] J. Wang, Q. W. Ma, S. Yan, and A. Chabchoub, Breather Rogue Waves in Random Seas, Phys. Rev. Appl. **9**, 014016 (2018).

[17] A. Chabchoub, N. Hoffmann, M. Onorato, and N. Akhmediev, Super Rogue Waves: Observation of a Higher-Order Breather in Water Waves, Phys. Rev. X **2**, 011015 (2012).

[18] S. Flach, K. Kladko, and S. Takeno, Acoustic Breathers in Two-Dimensional Lattices, Phys. Rev. Lett. **79**, 4838 (1997).

[19] H. Bailung, S. K. Sharma, and Y. Nakamura, Observation of Peregrine Solitons in a Multicomponent Plasma with Negative Ions, Phys. Rev. Lett. **107**, 255005 (2011).

[20] A. Mussot, C. Naveau, M. Conforti, A. Kudlinski, F. Copie, P. Szriftgiser, and S. Trillo, Fibre multi-wave mixing combs reveal the broken symmetry of Fermi–Pasta–Ulam recurrence, Nat. Photonics **12**, 303 (2018).

[21] G. Xu, A. Gelash, A. Chabchoub, V. Zakharov, and B. Kibler, Breather Wave Molecules, Phys. Rev. Lett. **122**, 084101 (2019).

[22] V. I. Shrira and V. V. Geogjaev, What makes the Peregrine soliton so special as a prototype of freak waves?, J. Eng. Math. **67**, 11 (2010).

[23] B. Frisquet, B. Kibler, and G. Millot, Collision of Akhmediev Breathers in Nonlinear Fiber Optics, Phys. Rev. X **3**, 041032 (2013).

[24] P. Suret, R. El Koussaifi, A. Tikan, C. Evain, S. Randoux, C. Szwaj, and S. Bielawski, Single-shot observation of optical rogue waves in integrable turbulence using time microscopy, Nat. Commun. **7**, 13136 (2016).

[25] M. Närhi, B. Wetzel, C. Billet, S. Toenger, T. Sylvestre, J.-M. Merolla, R. Morandotti, F. Dias, G. Genty, and J. M. Dudley, Real-time measurements of spontaneous breathers and rogue wave events in optical fibre modulation instability, Nat. Commun. **7**, 13675 (2016).

[26] M. Bertola and A. Tovbis, Universality for the focusing nonlinear Schrödinger equation at the gradient catastrophe point: Rational breathers and poles of the tritronquée solution to Painlevé I, Commun. Pure Appl. Math. **66**, 678 (2013).

[27] P. Liao, K. Zou, C. Bao, A. Kordts, M. Karpov, M. H. P. Pfeiffer, L. Zhang, Y. Cao, A. Almaiman, F. Alishashi, A. Mohajerin-Ariaei, A. Fallahpour, M. Tur, T. J. Kippenberg, and A. E. Willner, in *Conference on Lasers and Electro-Optics*. (Optical Society of America, San Jose, California, 2018), p. JTh5A.4.

[28] M. Leonetti, C. Conti, and C. Lopez, Non-locality and collective emission in disordered lasing resonators, Light Sci. Appl. **2**, e88 (2013).

[29] K. Goda and B. Jalali, Dispersive Fourier transformation for fast continuous single-shot measurements, Nat. Photonics **7**, 102 (2013).

[30] F. Arecchi, G. Giacomelli, A. Lapucci, and R. Meucci, Two-dimensional representation of a delayed dynamical system, Phys. Rev. A **45**, R4225 (1992).

[31] D. Churkin, S. Sugavanam, N. Tarasov, S. Khorev, S. Smirnov, S. Kobtsev, and S. Turitsyn, Stochasticity, periodicity and localized light structures in partially mode-locked fibre lasers, Nat. Commun. **6**, 7004 (2015).

[32] A. F. Runge, C. Aguergaray, N. G. Broderick, and M. Erkintalo, Coherence and shot-to-shot spectral fluctuations in noise-like ultrafast fiber lasers, Opt. Lett. **38**, 4327 (2013).

[33] A. Mahjoubfar, D. V. Churkin, S. Barland, N. Broderick, S. K. Turitsyn, and B. Jalali, Time stretch and its applications, Nat. Photonics **11**, 341 (2017).

[34] G. Herink, B. Jalali, C. Ropers, and D. R. Solli, Resolving the build-up of femtosecond mode-locking with single-shot spectroscopy at 90MHz frame rate, Nat. Photonics **10**, 321 (2016).

[35] J. Peng and H. Zeng, Build-Up of Dissipative Optical Soliton Molecules via Diverse Soliton Interactions, Laser Photon. Rev. **12**, 1800009 (2018).

[36] X. Liu, X. Yao, and Y. Cui, Real-Time Observation of the Buildup of Soliton Molecules, Phys. Rev. Lett. **121**, 023905 (2018).

[37] J. Peng and H. Zeng, Triple-State Dissipative Soliton Laser Via Ultrafast Self-Parametric Amplification, Phys. Rev. Appl. **11**, 044068 (2019).

[38] A. F. Runge, N. G. Broderick, and M. Erkintalo, Observation of soliton explosions in a passively mode-locked fiber laser, Optica **2**, 36 (2015).

[39] K. Krupa, K. Nithyanandan, and P. Grelu, Vector dynamics of incoherent dissipative optical solitons, Optica **4**, 1239 (2017).

[40] M. Liu, A.-P. Luo, Y.-R. Yan, S. Hu, Y.-C. Liu, H. Cui, Z.-C. Luo, and W.-C. Xu, Successive soliton explosions in an ultrafast fiber laser, Opt. Lett. **41**, 1181 (2016).

[41] J. Peng and H. Zeng, Soliton collision induced explosions in a mode-locked fibre laser, Commun. Phys. **2**, 34 (2019).

[42] O. Svelto and D. C. Hanna, *Principles of Lasers* (Springer, New York, 1998).

[43] G. P. Agrawal, *Nonlinear Fiber Optics* (Academic press, New York, 2007).

[44] W. Liu, C. Li, Z. Zhang, F. X. Kärtner, and G. Chang, Self-phase modulation enabled, wavelength-tunable ultrafast fiber laser sources: an energy scalable approach, Opt. Express **24**, 15328 (2016).

[45] C. Hönninger, R. Paschotta, F. Morier-Genoud, M. Moser, and U. Keller, Q-switching stability limits of continuous-wave passive mode locking, J. Opt. Soc. Am. B **16**, 46 (1999).

[46] T. Kolokolnikov, M. Nizette, T. Erneux, N. Joly, and S. Bielawski, The Q-switching instability in passively mode-locked lasers, Physica D **219**, 13 (2006).

[47] M. Liu, A.-P. Luo, W.-C. Xu, and Z.-C. Luo, Dissipative rogue waves induced by soliton explosions in an ultrafast fiber laser, Opt. Lett. **41**, 3912 (2016).

[48] D. Solli, C. Ropers, P. Koonath, and B. Jalali, Optical rogue waves, Nature **450**, 1054 (2007).

[49] C. Lecaplain and P. Grelu, Rogue waves among noiselike-pulse laser emission: an experimental investigation, Phys. Rev. A **90**, 013805 (2014).
[50] C. Lecaplain, J. M. Soto-Crespo, P. Grelu, and C. Conti, Dissipative shock waves in all-normal-dispersion mode-locked fiber lasers, Opt. Lett. **39**, 263 (2014).
[51] F. W. Wise, A. Chong, and W. H. Renninger, High-energy femtosecond fiber lasers based on pulse propagation at normal dispersion, Laser Photon. Rev. **2**, 58 (2008).
[52] W. H. Renninger, A. Chong, and F. W. Wise, Giant-chirp oscillators for short-pulse fiber amplifiers, Opt. Lett. **33**, 3025 (2008).
[53] N. Joly and S. Bielawski, Suppression of Q-switch instabilities by feedback control in passively mode-locked lasers, Opt. Lett. **26**, 692 (2001).
[54] T. Schibli, U. Morgner, and F. Kärtner, Control of Q-switched mode locking by active feedback, Opt. Lett. **26**, 148 (2001).
[55] B. Oktem, C. Ulgudur, and F. O. Ilday, Soliton-similariton fibre laser, Nat. Photonics **4**, 307 (2010).
[56] M. Nakazawa, M. Yoshida, and T. Hirooka, The Nyquist laser, Optica **1**, 15 (2014).
[57] T. J. Kippenberg, A. L. Gaeta, M. Lipson, and M. L. Gorodetsky, Dissipative Kerr solitons in optical microresonators, Science **361**, eaan8083 (2018).